Catalysis Today 147S (2009) S156–S161

Contents lists available at ScienceDirect

Catalysis Today

journal homepage: www.elsevier.com/locate/cattod

A novel catalytic-homogenous micro-combustor

Almerinda Di Benedetto [a,*], Valeria Di Sarli [a], Gennaro Russo [b]

[a] Istituto di Ricerche sulla Combustione, Consiglio Nazionale delle Ricerche (CNR), Via Diocleziano 328, 80124, Naples, Italy
[b] Dipartimento di Ingegneria Chimica, Università degli Studi di Napoli Federico II, Piazzale Tecchio 80, 80125, Naples, Italy

ARTICLE INFO

Article history:
Available online 5 August 2009

Keywords:
Catalytic micro-combustors
CFD
Thermal power

ABSTRACT

Miniaturizing combustors from macro- down to micro-scales leads to an increase of the surface area to volume ratio and, thus, thermal and radical quenching may prevail. The ranges of operating conditions at which micro-combustors exhibit stable behaviors are very narrow unless a catalyst is employed. However, catalytic combustors face the problems of thermal control related to the formation of hot spots and the subsequent catalyst deactivation.

In this paper, two-dimensional computational fluid dynamics (CFD) simulations are run to investigate into the opportunity of setting up a novel scheme of micro-combustor divided into two parts. In the first part, the walls of the micro-combustor are catalyst-coated, while in the second part, the catalyst is absent and only homogenous combustion can take place.

Numerical results show that this hybrid micro-combustor (HμC) allows operating at high inlet gas velocities and thus high input powers, without encountering blow-out and maintaining almost complete fuel conversions. This enlargement effect of the operating map on the high inlet velocity side increases on increasing the solid thermal conductivity. Furthermore, the catalytic wall temperature of such HμC is controlled and taken below 1200 K, thus preserving the catalyst.

1. Introduction

Owing to their high specific energy (45 kJ/g), micro-combustors may substitute traditional lithium batteries (specific energy = 1.2 kJ/g) in micro-electromechanical systems (MEMS) [1].

When scaling down from macro- to micro-reactors, phenomena negligible at the macro-scales become relevant at the micro-scales. Miniaturizing macro-combustors leads to an increase of the surface area to volume ratio and, thus, thermal and radical quenching may prevail [1–6]. It has been shown that the ranges of operating conditions at which micro-combustors exhibit stable behaviors are very narrow [3–6]. Conversely, catalytic micro-combustors exhibit wider stability maps than homogenous micro-combustors [7,8]. The catalytic layer deposited on the reactor walls may allow sustaining chemical reactions at lower temperatures and in the presence of higher heat losses, thus reducing the impact of thermal quenching.

However, catalytic micro-combustors face the problems of thermal control related to hot spots, traveling heat waves and wrong way behaviors, which all lead to the catalyst deactivation. Furthermore, the use of micro-combustors for MEMS requires high power density, which can be obtained by increasing the inlet mass flow rate and thus gas velocity. On the other hand, to reach high conversions, the residence time should be relatively high which means that low inlet gas velocities are needed to prevent blow-out conditions. As a result, a trade-off in the choice of the inlet gas velocity has to be reached.

In this framework, it would be beneficial to define a novel reactor configuration in which combustion is stabilized also at high inlet gas velocities with complete conversions.

By means of numerical simulations, we have shown that it is possible to operate a catalytic micro-combustor, fed with lean propane–air mixtures, at high inlet gas velocities (i.e., up to the velocity value limiting the laminar regime for the incoming flow, ~100 m/s for the geometry investigated) with wall temperatures higher than gas temperatures (1600 K *versus* 800 K) and fuel conversions of around 30% [9].

Based on these results, in this paper, we present a novel scheme of micro-combustor divided into two parts. In the first part, the walls of the micro-combustor are catalyst-coated, while in the second part, the catalyst is absent and only homogenous combustion can take place.

In such hybrid micro-combustor (HμC), the catalytic part is used to provide light-off. The heat generated at the catalytic walls is transferred downstream by conduction. This allows both the cooling of the catalytic walls and the preheating of the walls of the

* Corresponding author.
E-mail addresses: almerinda.dibenedetto@irc.cnr.it (A. Di Benedetto), valeria.disarli@irc.cnr.it (V. Di Sarli), genrusso@unina.it (G. Russo).

0920-5861/$ – see front matter © 2009 Elsevier B.V. All rights reserved.
doi:10.1016/j.cattod.2009.07.030

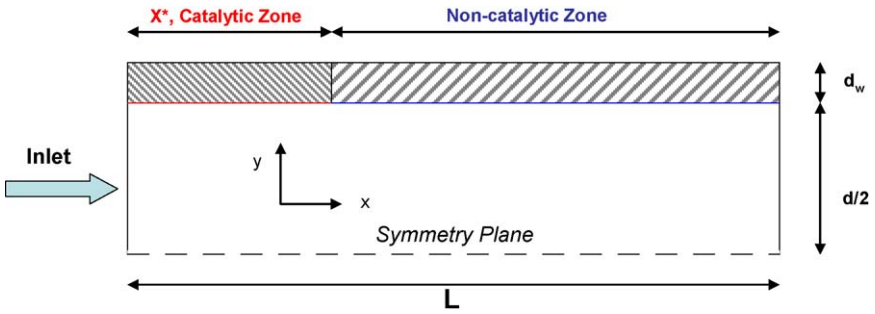

Fig. 1. Scheme of the hybrid micro-combustor (parallel plate reactor). The dashed line is the axis of symmetry.

homogenous section, where volumetric combustion is stabilized, thus completing fuel (propane) conversions.

The opportunity of setting up the HμC scheme is investigated by means of computational fluid dynamics (CFD) simulations.

2. The model

A two-dimensional CFD model is developed to simulate the coupling of the fluid flow and the chemical processes at the gas–solid interface and in the gas phase.

In Fig. 1, the scheme of the hybrid micro-combustor (HμC) is shown which consists of two parallel (infinitely wide) plates (gap distance, d = 600 μm; wall thickness, d_w = 200 μm; length of the catalytic zone, X^* = 0.01 m; total length, L = 0.06 m).

The model solves the mass, momentum, species and energy conservation equations in the fluid along with the energy equation in the solid wall. Steady-state simulations are carried out.

The conservation equations in the fluid are listed below (conventional notation is adopted):

Continuity

$$v_x\frac{\partial\rho}{\partial x}+v_y\frac{\partial\rho}{\partial y}+\rho\left(\frac{\partial v_x}{\partial x}+\frac{\partial v_y}{\partial y}\right)=0 \tag{1}$$

Momentum

$$\frac{\partial\rho v_x v_x}{\partial x}+\frac{\partial\rho v_x v_y}{\partial y}=-\frac{\partial p}{\partial x}+\frac{\partial\tau_{xx}}{\partial x}+\frac{\partial\tau_{yx}}{\partial y} \tag{2}$$

$$\frac{\partial\rho v_x v_y}{\partial x}+\frac{\partial\rho v_y v_y}{\partial y}=-\frac{\partial p}{\partial y}+\frac{\partial\tau_{xy}}{\partial x}+\frac{\partial\tau_{yy}}{\partial y} \tag{3}$$

Species (i = 1, …, N_s − 1, with N_s species number)

$$\frac{\partial\rho v_x Y_i}{\partial x}+\frac{\partial\rho v_y Y_i}{\partial y}=\frac{\partial}{\partial x}\left(\rho D_{i,m}\frac{\partial Y_i}{\partial x}\right)+\frac{\partial}{\partial y}\left(\rho D_{i,m}\frac{\partial Y_i}{\partial y}\right)+R_i \tag{4}$$

Energy

$$\frac{\partial\rho v_x h}{\partial x}+\frac{\partial\rho v_y h}{\partial y}=\frac{\partial}{\partial x}\left(\lambda\frac{\partial T}{\partial x}\right)+\frac{\partial}{\partial y}\left(\lambda\frac{\partial T}{\partial y}\right)+\sum_{i=1}^{N_S}\left(\frac{\partial(h_i\rho D_{i,m}\partial Y_i/\partial x)}{\partial x}+\frac{\partial(h_i\rho D_{i,m}\partial Y_i/\partial y)}{\partial y}\right)-\sum_{i=1}^{N_S}h_i R_i \tag{5}$$

The above equations are coupled to the ideal-gas equation:

$$\rho=\frac{pW_{\mathrm{mix}}}{\Re T} \tag{6}$$

The energy equation in the solid wall reads:

$$0=\lambda_w\left(\frac{\partial^2 T_w}{\partial x^2}+\frac{\partial^2 T_w}{\partial y^2}\right) \tag{7}$$

where λ_w is the solid thermal conductivity.

At the inlet of the micro-combustor, a fixed flat velocity profile is assumed. For species and energy, Danckwerts boundary conditions are used. At the exit, the static pressure is imposed as equal to the atmospheric pressure, and far-field conditions are specified for the remaining variables. At the fluid-wall interface, a no-slip boundary condition is assigned (the fluid has zero velocity relative to the boundary) which, in the catalytic zone, is coupled to the species balances (the mass flux of each species, ρJ_i, is equal to its rate of production/consumption, $\omega_{y,i}$):

$$\rho J_i=\omega_{y,i} \tag{8}$$

and the energy balance:

$$\lambda\frac{\partial T}{\partial y}=\lambda_w\frac{\partial T_w}{\partial y}+\omega_{\mathrm{h}} \tag{9}$$

where ω_{h} is the heat surface production rate.

Heat losses from the ends of the micro-combustor are not considered (insulated ends), while Newton's law of convection is used at the outer surface of the wall:

$$q=h(T_{w,\mathrm{ext}}-T_{a,\mathrm{ext}}) \tag{10}$$

where h is the exterior convective heat transfer coefficient, $T_{w,\mathrm{ext}}$ is the temperature at the exterior wall surface, and $T_{a,\mathrm{ext}}$ is the external temperature (=300 K).

The reaction rate for homogenous propane combustion is calculated according to the single-step reaction rate by Westbrook and Dryer [10]:

$$R_H=4.836E+9\cdot\exp\left(\frac{-1.256E+8}{\Re T}\right)\cdot(C_{C_3H_8})^{0.1}(C_{O_2})^{1.65}\left[\frac{\mathrm{kmol}}{\mathrm{m^3\,s}}\right] \tag{11}$$

where the activation energy is in J/kmol and the concentrations in kmol/m^3.

The catalytic reaction is assumed to be irreversible, first order in fuel concentration and zeroth order in oxygen concentration [11]. The reaction rate, referred to platinum as the catalyst, is calculated according to:

$$R_C=2.4E+5\cdot\exp\left(\frac{-9.06E+7}{\Re T}\right)\cdot C_{C_3H_8}\left[\frac{\mathrm{kmol}}{\mathrm{m^2\,s}}\right] \tag{12}$$

where the activation energy is in J/kmol and the concentration in kmol/m^2.

The molecular viscosity is approximated through Sutherland's law for air viscosity. The fluid specific heat and thermal conductivity are calculated by a mass fraction weighted average of species properties. The species specific heat is evaluated as a piecewise fifth-power polynomial function of temperature.

The model equations are discretised using a finite volume formulation on a structured mesh built by means of the Gambit pre-processor of the Fluent package (version 6.3.26) [12]. Grid

Table 1
Conditions adopted.

Parameter	Value
Inlet gas temperature, T_{in} (K)	300
Inlet gas velocity, v_{in} (m/s)	0.2–30
Inlet fuel equivalence ratio, ϕ	0.6
Exterior convective heat transfer coefficient, h (W/m^2 K)	20
Solid thermal conductivity, λ_w (W/m K)	2; 20

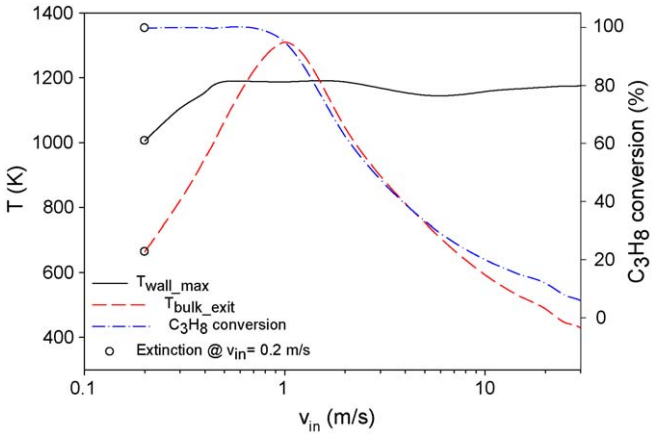

Fig. 2. Stability map of the micro-combustor with only the catalytic section (length equal to 0.01 m and λ_w = 2 W/m K).

independent solutions are found using cells with a dimension equal to 2.5 E−2 mm.

The spatial discretization of the model equations uses first order schemes for all terms, except for the diffusion terms that are treated with a second order central difference scheme.

Computations are performed by means of the segregated solver of the Fluent code [12] that adopts the SIMPLE method for treating the pressure–velocity coupling. All residuals are always smaller than 1.0 E−7.

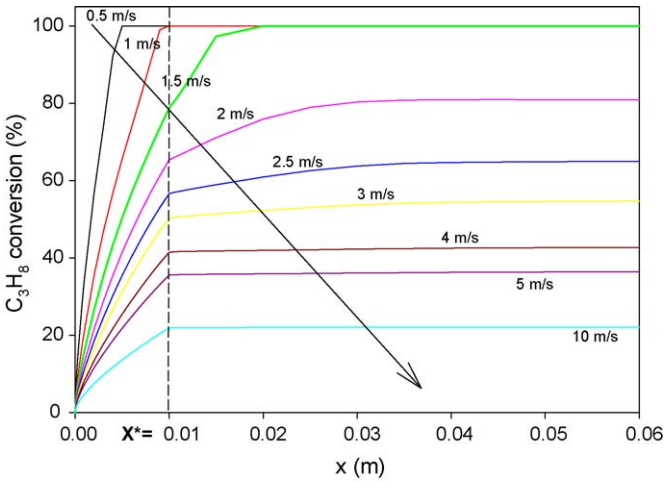

Fig. 3. Propane conversion as a function of the axial coordinate at different inlet gas velocities. Hybrid micro-combustor with λ_w = 2 W/m K.

Simulations are also run of the micro-reactor with only the catalytic part (of length equal to 0.01 m), and the corresponding results are first presented in the next section.

Table 1 summarizes the operating conditions adopted in the computations.

3. Results and discussion

In Fig. 2, the stability map of the micro-combustor with only the catalytic section (catalytic micro-combustor, CμC, of length equal to 0.01 m and with λ_w = 2 W/m K) is shown terms of maximum wall temperature, T_{wall_max}, bulk gas temperature at the exit section, T_{bulk_exit}, and propane conversion *versus* the inlet gas velocity, v_{in}.

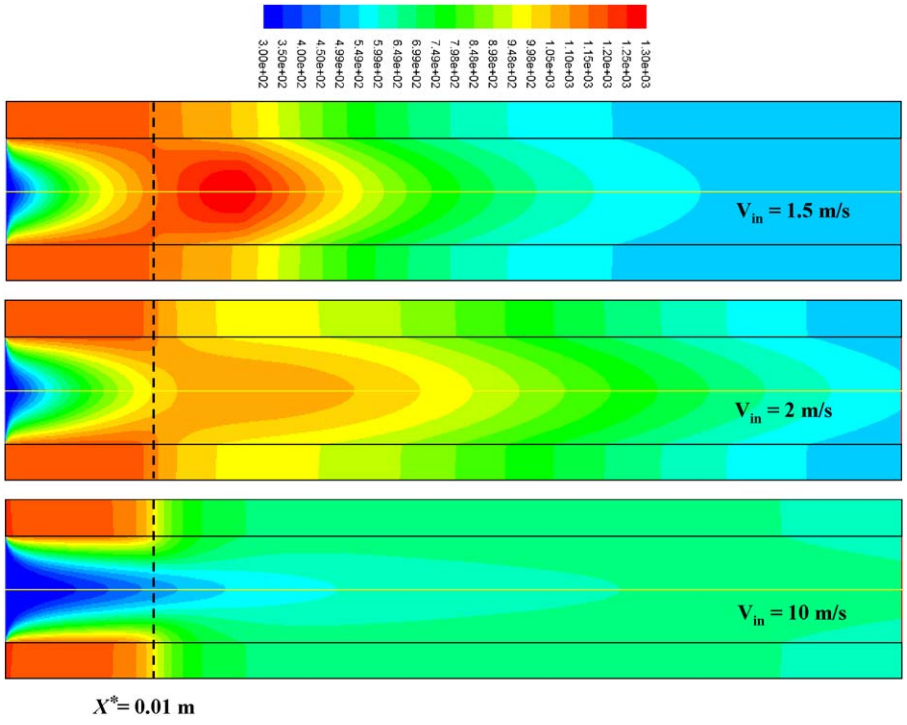

Fig. 4. Temperature (K) maps at different inlet gas velocities. Hybrid micro-combustor with λ_w = 2 W/m K.

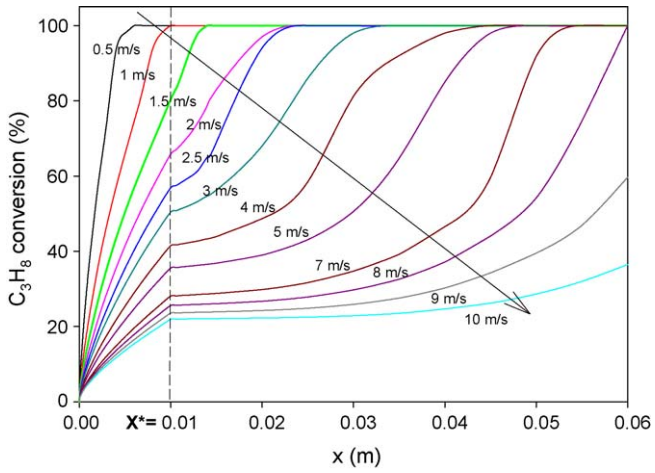

Fig. 5. Propane conversion as a function of the axial coordinate at different inlet gas velocities. Hybrid micro-combustor with λ_w = 20 W/m K.

At low inlet gas velocities ($v_{in} < 1$ m/s), high propane conversions (≈100%) are attained. At higher inlet gas velocities ($v_{in} > 1$ m/s), the propane conversion decreases, but the wall temperature is still high (order of 1200 K) and higher than the bulk gas temperature.

The hybrid micro-combustor (HμC) is supposed to operate at high inlet gas velocities (i.e., at high input powers). It should take advantage of high wall temperatures (1200 K) in the first zone to stabilize homogeneous combustion at high inlet gas velocities in the second zone.

In Fig. 3, the propane conversion, as calculated for the HμC with λ_w = 2 W/m K, is plotted *versus* the axial coordinate at different inlet gas velocities.

It is shown that, at low inlet gas velocities ($v_{in} \leq 1$ m/s), complete propane conversions are attained in the catalytic zone ($x \leq X^*$ = 0.01 m) and, consequently, the homogeneous part of the micro-combustor is useless. However, at higher inlet gas velocity ($v_{in} > 1$ m/s) and thus higher input power, the homogeneous part allows increasing the propane conversion.

At v_{in} = 1.5 m/s, the value of propane conversion at the exit of the catalytic part is equal to 78%. This value increases up to 100% at the exit of the downstream homogeneous zone. At higher inlet gas velocities ($v_{in} > 1.5$ m/s), increments of propane conversion are still observed, but conversions remain far from 100%.

Fig. 4 shows the temperature maps as computed at v_{in} = 1.5, 2 and 10 m/s for the HμC.

For the case v_{in} = 1.5 m/s, the hot spot downstream of the catalytic zone ($x \geq X^*$ = 0.01 m) demonstrates that, within the second part of the micro-combustor, the volumetric reaction process is occurring. However, this homogeneous section is not appropriately used, the most of it being cold (with wall temperature decreasing down to around 500 K), and acting as a heat exchanger rather than as a chemical reactor.

Fig. 4 also shows that, on increasing the inlet gas velocity, the homogeneous reaction rate decreases and blow-out occurs as a consequence of the coupling between cold walls and low residence time of the gas.

The activation and stabilization of homogeneous reaction in the second part of the micro-combustor depend on the temperature level attained in this zone and, thus, on the heat transferred through the walls from the upstream catalytic section to the downstream homogeneous section.

In order to test the role of the axial heat flux through the wall (conductive heat flux) in activating and stabilizing the homogeneous combustion process, the effect of the wall thermal conductivity is investigated.

In Fig. 5, the axial profiles of propane conversion are shown as obtained along the HμC with λ_w = 20 W/m K, at varying the inlet gas velocity.

It can be noted that the range of inlet gas velocities at which the HμC provides propane conversions higher than 95%, extends from 0.5 to 8 m/s. Conversely, with the HμC @ λ_w = 2 W/m K, this range is much narrower (0.5–1.5 m/s) (Fig. 3).

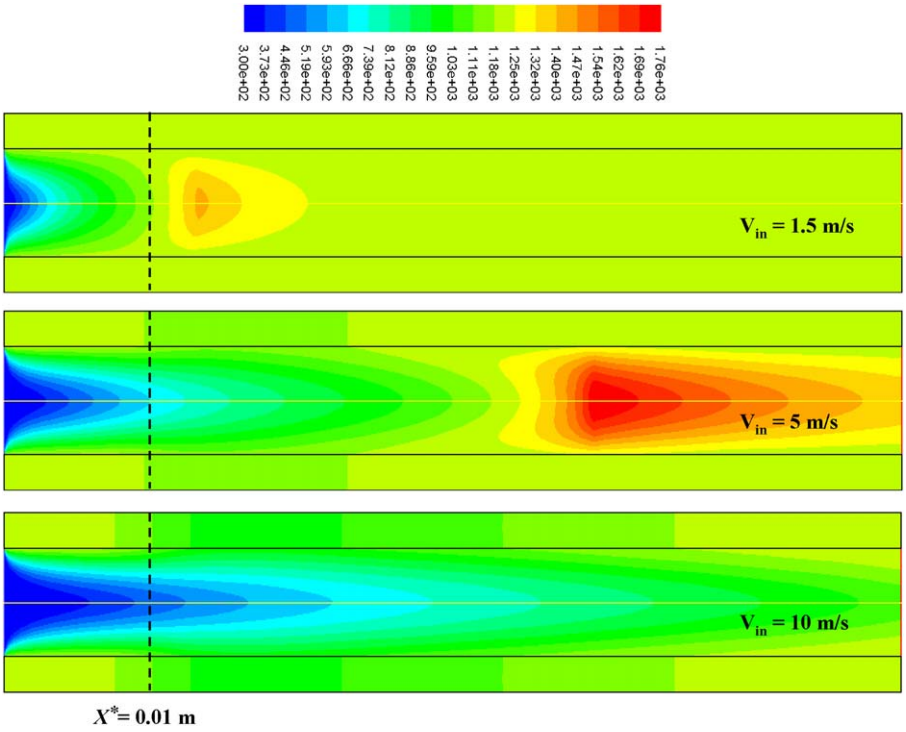

Fig. 6. Temperature (K) maps at different inlet gas velocities. Hybrid micro-combustor with λ_w = 20 W/m K.

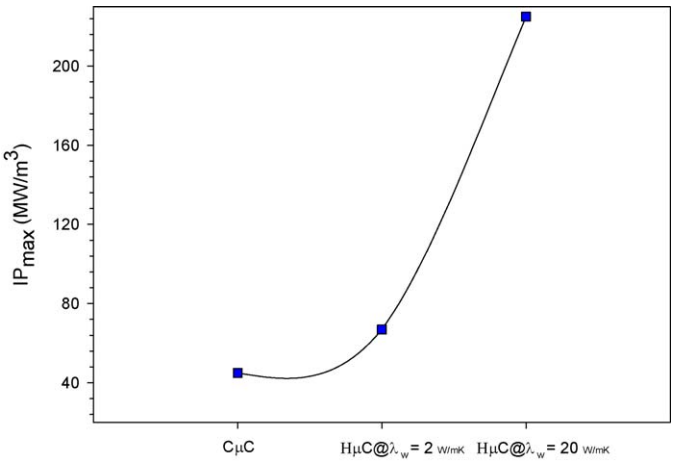

Fig. 7. Maximum input power density as obtained for three configurations: CμC @ λ_w = 2 W/m K; HμC @ λ_w = 2 W/m K and HμC @ λ_w = 20 W/m K.

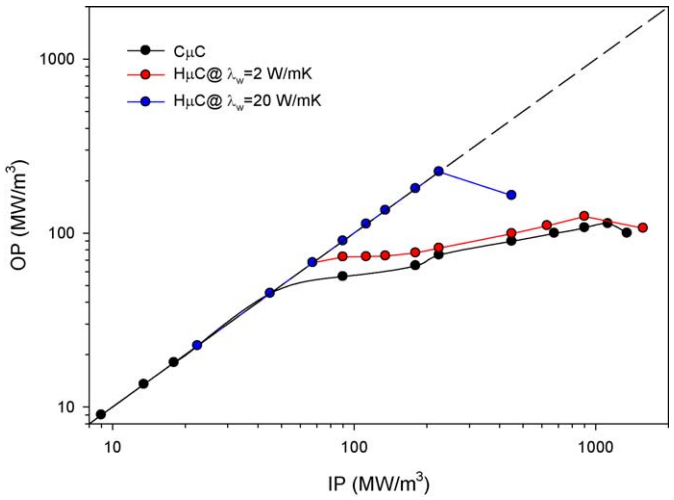

Fig. 8. Output power density as a function of the input power density for three configurations: CμC @ λ_w = 2 W/m K; HμC @ λ_w = 2 W/m K and HμC @ λ_w = 20 W/m K. The line OP = IP is also shown (dashed line).

The significant enlargement of the operating region at λ_w = 20 W/m K is related to the higher amount of heat diffused from the catalytic zone, which heats up the walls, to the homogeneous zone.

Fig. 6 shows the temperature maps as computed at v_{in} = 1.5, 5 and 10 m/s for the HμC with λ_w = 20 W/m K.

The temperature gradients within the solid wall are now much less steep than those found with λ_w = 2 W/m K (Fig. 4). On increasing the inlet gas velocity, the homogeneous reaction front is shifted downstream (v_{in} = 5 m/s) and then blown-out (v_{in} = 10 m/s).

3.1. Operating diagrams

The operating conditions of micro-combustors should satisfy both combustion efficiency and material stability criteria at high input power density.

Combustion efficiency is attained with complete conversions, while material is preserved if the catalyst-coated wall temperature is lower than a threshold value that depends on the material type.

For the configurations investigated:

1. Catalytic micro-combustor (CμC)
2. HμC @ λ_w = 2 W/m K
3. HμC @ λ_w = 20 W/m K

the input power density, IP, is calculated according to the following formula:

$$\mathrm{IP} = \frac{m_{C_3H_8}|\Delta H_c|}{V} \quad (13)$$

where $m_{C_3H_8}$ is the propane mass flow rate fed to the reactor, ΔH_c is the heat of combustion, and V is the volume of the reactor.

The maximum input power density, IP_{max}, is also computed at the maximum propane mass flow rate (i.e., at the maximum inlet gas velocity) at which the outlet propane conversion is still higher than 95%. In Fig. 7, IP_{max} is reported for configurations 1–3.

It is shown that the hybrid micro-combustor with high wall thermal conductivity (HμC @ λ_w = 20 W/m K) may operate up to 225 MW/m^3, while with lower thermal conductivity (HμC @ λ_w = 2 W/m K), the maximum input power density is equal to 67 MW/m^3. This value is similar to that attainable in the absence of the second homogeneous part (CμC, 45 MW/m^3).

The output power density, OP, as obtained multiplying the input power density by the outlet propane conversion ($\mathrm{OP} = \mathrm{IP}x_{C_3H_8}$), is plotted in Fig. 8 as a function of IP. The line OP = IP is also shown in this figure (dashed line).

When points overlap the line OP = IP, the outlet propane conversion is complete. On increasing the input power density (i.e., on increasing the inlet gas velocity), the propane conversion decreases and OP becomes lower than IP.

The highest output power density is obtained with configuration 3 (HμC @ λ_w = 20). Configurations 1 and 2 allow reaching high output power density (up to 120 MW/m^3), but at much higher input power density (i.e., at lower propane conversion).

It is worth noting that, in all conditions investigated in the present work, the maximum catalyst-coated wall temperature is lower than 1200 K, thus ensuring material stability.

4. Conclusions

In this paper, CFD simulations have been run to investigate into the opportunity of enlarging the operating region of a micro-combustor on the high inlet velocity side.

A novel scheme of hybrid micro-combustor has been proposed consisting of two parts: a first catalytic part, and a second non-catalytic (homogenous) part. This first part provides light-off. Within the second part, the homogeneous reaction process is stabilized owing to the heat diffusing from the catalytic zone downstream through the walls.

Numerical results have shown that the HμC allows operating at high inlet gas velocities, without encountering blow-out and maintaining high fuel conversions. This enlargement effect of the operating map increases on increasing the solid thermal conductivity. Furthermore, the catalytic wall temperature of such HμC is always below 1200 K, thus preserving the catalyst.

In conclusion, it has been shown that the HμC is a promising reactor scheme for stabilizing micro-combustion in wide ranges of input power with complete fuel conversions.

Acknowledgments

The authors wish to thank Dott. V. Smiglio for his technical assistance in the computing activity.

References

[1] A.C. Fernandez-Pello, Proc. Combust. Inst. 29 (2002) 883–899.
[2] P. Aghalayam, D.G. Vlachos, AIChE J. 44 (1998) 2025–2034.

[3] S. Raimondeau, D. Norton, D.G. Vlachos, R.I. Masel, Proc. Combust. Inst. 29 (2002) 901–907.
[4] D.G. Norton, D.G. Vlachos, Chem. Eng. Sci. 58 (2003) 4871–4882.
[5] D.G. Norton, D.G. Vlachos, Combust. Flame 138 (2004) 97–107.
[6] C.M. Spadaccini, A. Mehra, J. Lee, X. Zhang, S. Lukachko, I.A. Waitz, J. Eng. Gas Turb. Power 125 (2003) 709–719.
[7] N.S. Kaisare, S.R. Deshmukh, D.G. Vlachos, Chem. Eng. Sci. 63 (2008) 1098–1116.
[8] K. Maruta, K. Takeda, J. Ahn, K. Borer, L. Sitzki, P.D. Ronney, O. Deutschmann, Proc. Combust. Inst. 29 (2002) 957–963.
[9] A. Di Benedetto, V. Di Sarli, G. Russo, Catal. Today (2009), doi:10.1016/j.cattod.2009.01.048.
[10] C. Westbrook, F. Dryer, Combust. Sci. Technol. 27 (1981) 31–43.
[11] C.M. Spadaccini, J. Peck, I.A. Waitz, J. Eng. Gas Turb. Power 129 (2007) 49–60.
[12] Fluent (version 6.3.26), Fluent Inc. http://www.fluent.com, 2008 (accessed 25.03.09).